Preprints of the 19th World Congress
The International Federation of Automatic Control
Cape Town, South Africa. August 24-29, 2014

Distributed Generation System Control Strategies in Microgrid Operation

Wenlei Bai* and Kwang Lee**

*Baylor University, Waco, TX 76706
USA (Tel: 254-405-3320; e-mail: Wenlei_Bai@baylor.edu).
**Baylor University, Waco, TX 76706 USA (e-mail:
Kwang_Y_Lee@baylor.edu).

Abstract: Control strategies of distributed generation (DG) are investigated for different combination of DG and storage units in a microgrid. This paper develops a detailed photovoltaic (PV) array model with maximum power point tracking (MPPT) control, and presents real and reactive power (PQ) control and droop control for DG system for microgrid operation. In grid-connected mode, PQ control is developed by controlling the active and reactive power output of DGs in accordance with assigned references. In islanded mode, DGs are controlled by droop control. Droop control implements power reallocation between DGs based on predefined droop characteristics whenever load changes or the microgrid is connected/disconnected to the grid, while the microgrid voltage and frequency is maintained at appropriate levels. This paper presents results from a test microgrid system consisting of a voltage source converter (VSC) interfacing with a DG, a PV array with MPPT, and changeable loads. The control strategies are tested via two scenarios: the first one is to switch between grid-connected mode and islanded mode and the second one is to change loads in islanded mode. Through voltage, frequency, and power characteristics in the simulation under such two scenarios, the proposed control strategies can be demonstrated to work properly and effectively.

Keywords: Distributed generation, PV, Microgrid, Droop control, PQ control.

1. INTRODUCTION

A microgrid is a system that aggregates generators, consumers, energy storage devices and hybrid devices such as electric vehicles which are able to both produce and consume energy. Microgrid can generally be viewed as a cluster of distributed generators (DGs) connected to the main utility grid, usually through voltage source converter (VSC) based interfaces (Cho et al., 2011). Distributed generation (DG) technologies are the main part in microgrid and has been placed much emphasis because these technologies produce energy with less environmental impact, easy to site, and are highly efficient (Puttgen, Macgregor and Lambert, 2003).

DGs encompass a wide range of prime-mover technologies, such as internal combustion engines, gas turbines, wind power, micro turbines, photovaltaics (PV), fuel cells, etc. But controlling a potentially huge number of DGs creates a daunting new challenge for operating and controlling the network safely and efficiently (Hatziargyriou et al., 2007). This challenge can be partially addressed by microgrids. Microgrid can operate in two modes: grid-connected mode and island mode. In normal grid-connected mode power will be supplied to loads either though the main grid or the microgrid; however when there is a failure in the grid, microgrid will disconnect from the grid and operate in island mode.

Different from traditional utility grid, a microgrid contains DGs through VSC to interface with utility. The VSC have more controlled variables than the commonly used synchronous generators (Tan, So and Chu, 2010). Thus one of the key problems in microgrid operation is to determine control strategies. When loads change or disconnection occurs, controllers need to coordinate DGs to guarantee power quality and demand in the microgrid. In (Cai and Mitra, 2010), decentralized control using multi-agent systems approach is proposed by using only the local information of DGs. The decentralized architecture of the microgrid is equipped with power electronic interfaces and all the agents are equal and autonomous, and they only communicate with their neighbours to achieve power balancing and thus maintain voltage and frequency. However this method requires large amount of communication which increases the complexity when implemented for control.

In (Barsali et al.,2002) voltage and frequency (V/f) control was proposed to control DGs in island mode by maintaining voltage and frequency at references. However pure V/f controller for DGs in islanded mode is not able to respond to load changes, thus in (Chen, Wang and Wang, 2013), a master-slave control configuration of a microgrid is proposed. In grid-connected mode all DGs are equipped with PQ controllers, and under islanded mode only the master inverter switches to V/f control to maintain the microgrid voltage level and frequency. The drawback of master-slave method is that it also takes large amount of communication. In practical microgrid operation, controllers for different

types of DGs vary extensively. For example, micro turbines and fuel cell can be equipped with either PQ controller in order to follow real and reactive power references or V/f controller which maintains stability of microgrid's voltage and frequency; however for renewable energy DGs such as wind turbine and PV, due to their intermittence, PQ controller will have to be used to maximize renewable energy.

In order to operate microgrid under both modes effectively by satisfying the load demand and voltage/frequency stability, while minimizing the communication between DGs in microgrid control, a PQ controller and droop controller is proposed in this paper. The control strategies presented here is to overcome the drawback of pure V/f control which leads to the failure of responding to load changes and the drawback of master-slave control which requires certain amount of DG communication. The use of droop characteristics concepts is commonly used in controlling generating units in power system (Kundur, 1993). In terms of the interfacing a microgrid to the utility grid, DGs should achieve proper load sharing. A load sharing with minimal communication is the best because of the complexity of network system and thus droop control method is presented in this paper. Both PV and DG were carried out with PQ control in grid-connection mode, while they were switched into droop control once disconnected from the grid. A detailed PV model with MPPT control is also developed and formed a parallel-inverter based microgrid in which there is one PV and another DG in this paper.

The paper is organized as follows: Section II describes the proposed architecture of the microgrid. Section III describes PV model and controller design process. In Section IV the performance of the proposed controller is tested and results are shown in simulation. Finally the conclusion is provided in Section V with recommendation for future works.

2. MICROGRID ARCHITECTURE

In order to test the effectiveness and efficiency of controllers, a microgrid structure is proposed as shown in Fig. 1. The microgrid contains one PV array and one other DG. DGs in microgrid can be fuel cells, PV, wind turbines or energy storage system, etc. The PV provides DC power, and MPPT was implemented to obtain the maximum power output in the project.

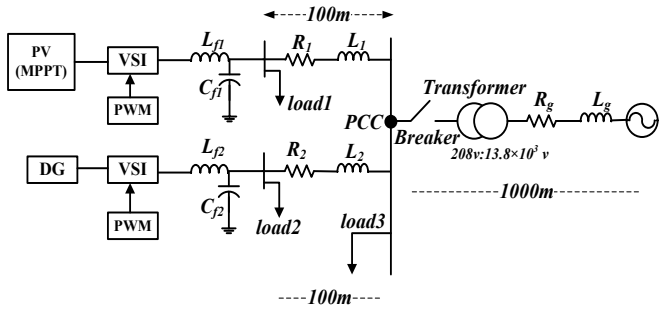

Fig. 1. Schematic of the microgrid.

In Fig. 1, PV and DG are connected to voltage source inverters (VSI) controlled by pulse width modulation (PWM). VSI converts DC voltage to AC voltage and then power go through low pass LC filter to filter high frequency noise. Load 1 and load 2 are connected to PV and DG after filters, respectively, and load 3 is connected at the point of common coupling (PCC). DGs are connected to the main grid through transmission line, switches and transformers. The distances from load 1 and 2 to PCC are 100 (m) and from PCC to main grid is 1000 (m). The tap ratio of transformer is $208:13.8\times10^3$ (v). Note that both PV and DG implement PQ controller under grid connection mode and droop controller under island mode. In this paper PV was modelled as the current source in parallel with an ideal diode, and the other DG was modelled as a constant DC voltage source for simplicity.

3. PV MODEL AND CONTROLLER DESIGN

3.1 PV Model

A solar cell is the main component of a solar panel. A photovoltaic module is formed by connecting many solar cells in series and parallel, and a single solar cell can be modelled as a current source connecting with one diode and two resistors (Fig. 2).

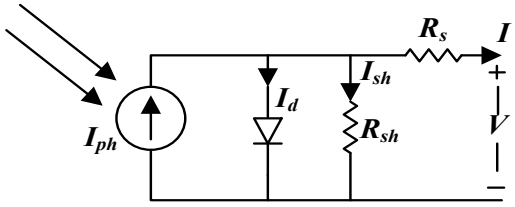

Fig. 2. Single diode model of a solar cell.

The characteristic equation for a single solar cell is given by (Villalva, Gazoli and Ruppert, 2009):

$$I = I_{ph} - I_0\left\{\exp\left[\frac{q(V+R_sI)}{nkT}\right]-1\right\} - \frac{V+R_sI}{R_{sh}} \quad (1)$$

Where I is output current, V is output voltage, I_0 is cell reverse saturation current, I_{ph} is light-generated current, q is electron charge, 1.6×10^{-23} (C), T is cell temperature in Celsius, k is Boltzamann's constant, 1.38×10^{-19} (J/k), R_s is series resistance and R_{sh} is shunt resistance. For actual non-ideal diode, ideality factor n is introduced in the denominator of the exponent, which ranges from1-2, representing the defects from ideal diode.

The P-V and I-V curves are important two indicators to characterize properties of a solar cell. Fig. 3 shows the effect of solar irradiation variation (from 200 to 1000 (w/m^2)) on P-V and I-V curves for the solar cell used in this project.

As shown in Fig. 3, the higher is the solar irradiation, the higher would be the solar input to the solar cell, and hence power magnitude would increase for the same amount of voltage. This is due to the fact that when more sunlight incidents are on to the solar cell, the electrons are supplied

with higher excitation energy, thereby increasing the electron mobility and thus more power is generated (Saurav, 2012).

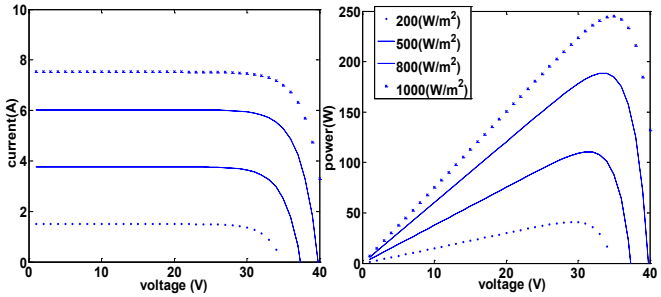

Fig. 3. P-V and I-V curves.

3.2 Maximum Power Point Tracking

The efficiency of a solar cell is very low. In order to increase the efficiency, methods are to be undertaken to match the source and load properly. One such method is the maximum power point tracking (MPPT). As P-V and I-V curves indicate in Fig. 3, when output voltage increases, power increases first and then drops, thus there exists a voltage corresponding to maximum power output. This voltage can be found and maintained by utilizing a boost converter whose duty cycle is controlled by the MPPT algorithm. Perturb and Observe (P&O) method (Ropp and Gonzalez 2009) is used to implement the MPPT, and the algorithm is based on the calculation of the PV array current and voltage.

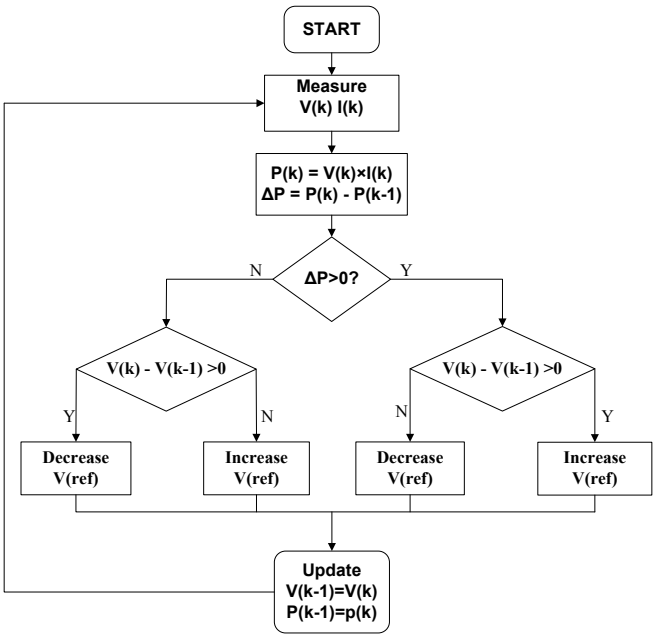

Fig. 4. The Perturb and Observe Method.

The P&O is demonstrated as a flow chart in Fig. 4. Given a voltage perturbation first, then $V(k)$ and $I(k)$ are sampled at time k, and then calculate power $P(k) = V(k)\times I(k)$. Compare $P(k)$ with $P(k-1)$, if power increases, keep searching in the same direction while power decreases, search the opposite direction to get final output voltage V. The P&O method leads to power oscillation about MPP, and reducing the voltage perturbation step size can minimize the oscillation. However, small step size slows down the MPPT. For different values of irradiance and cell temperatures, the PV array would exhibit different characteristic curves and each curve has its MPPT. The maximum voltage corresponding to this point is supplied to the converter as the reference voltage.

3.3 Controller Design

DG with PQ control is demonstrated in Fig. 5. Reference real power and reactive power are decoupled into reference current in d - and q -axis in 'Power Control' block, and then reference current are controlled by 'PI Current Controller' in order to make steady state error equal to zero. Phase Lock Loop (PLL) is used to synchronize frequency and phase of DG with main grid.

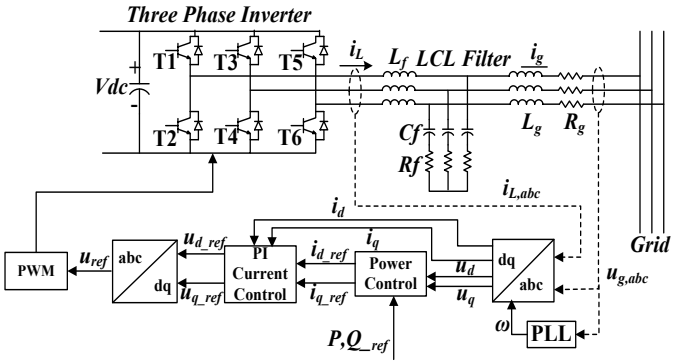

Fig. 5. Schematic of the PQ control.

In PQ control, the real and reactive power exchanged from the grid are the variables controlled by the inverter, and they have to meet the power reference. The three phase output voltage of inverter u can be represented as

$$\begin{bmatrix} u_a \\ u_b \\ u_c \end{bmatrix} = \begin{bmatrix} U_m \cos(\omega t) \\ U_m \cos(\omega t - \frac{2\pi}{3}) \\ U_m \cos(\omega t + \frac{2\pi}{3}) \end{bmatrix} \quad (2)$$

Where U_m is the maximum voltage magnitude of u, ω is the angular frequency. The three-phase stationary coordinate system can be transformed to d-q rotating coordinate system by Park transformation (Wu et al., 2011), and it is described as

$$T_{abc\to dq} = \frac{2}{3}\begin{bmatrix} \cos(\omega t) & \cos\left(\omega t - \frac{2\pi}{3}\right) & \cos\left(\omega t + \frac{2\pi}{3}\right) \\ \sin(\omega t) & \sin\left(\omega t - \frac{2\pi}{3}\right) & \sin\left(\omega t + \frac{2\pi}{3}\right) \end{bmatrix} \quad (3)$$

Then take Park's transformation on u to get:

$$\begin{bmatrix} u_d \\ u_q \end{bmatrix} = T_{abc\to dq} \begin{bmatrix} u_a \\ u_b \\ u_c \end{bmatrix} = \begin{bmatrix} U_m \\ 0 \end{bmatrix} \tag{4}$$

where u_d and u_q are the voltage under *d-q* coordinate system. Under stationary *abc* coordinate system, three phase voltage is coupled, while under rotating *d-q* rotating system, they are decoupled on *d*- and *q*-axis respectively (Sehirli and Altinay, 2012). In addition, u_d is a constant and u_q is zero (4). Thus the output current from inverter after Park's transformation can be calculated as (Chen, Wang and Wang, 2013)

$$\begin{aligned} i_{dref} &= \frac{P_{ref}}{u_d} \\ i_{qref} &= -\frac{Q_{ref}}{u_d} \end{aligned} \tag{5}$$

It is shown from (5) that the objective of controlling real and reactive power *P* and *Q* is equivalent to controlling current, in other words, as long as PQ controller implements tracking the current reference i_{ref}, both *P* and *Q* can be controlled. Current control is accomplished by PI controller.

Equation (6) gives the voltage equation of inverter in the rotating *d-q* reference frame (Choi and Sul, 1998):

$$\begin{bmatrix} u_d \\ u_q \end{bmatrix} = \begin{bmatrix} LS & \omega L \\ -\omega L & LS \end{bmatrix} \begin{bmatrix} i_d \\ i_q \end{bmatrix} + \begin{bmatrix} v_d \\ v_q \end{bmatrix} \tag{6}$$

where u_d and u_q are grid voltage, i_d and i_q are inverter current, *L* is filter inductance, v_d and v_q are control voltages.

It is shown from (6) that inverter current is coupled in terms of *d* and *q* axis, and i_d and i_q are not only affected by v_d and v_q but also the coupled voltage ωLi. Thus in order to control i_d and i_q independently, the coupled value needs to be cancelled, and current feed forward compensation is usually used. By introducing $-\omega Li_q$ and ωLi_d the current controller with PI control is written as:

$$\begin{bmatrix} v_d \\ v_q \end{bmatrix} = \begin{bmatrix} u_d \\ u_q \end{bmatrix} - \left(k_p + \frac{k_i}{S} \right) \begin{bmatrix} i_{d\_ref} \\ i_{q\_ref} \end{bmatrix} + \begin{bmatrix} -\omega L & 0 \\ 0 & \omega L \end{bmatrix} \begin{bmatrix} i_q \\ i_d \end{bmatrix} \tag{7}$$

Inserting (7) into (6), the relationship between reference control current and inverter current can be derived as:

$$\begin{bmatrix} i_{d\_ref} \\ i_{q\_ref} \end{bmatrix} = \left(\frac{LS}{k_p + \frac{k_i}{S}} + 1 \right) \begin{bmatrix} i_d \\ i_q \end{bmatrix} \tag{8}$$

From (8) we find that by introducing feed forward compensation reference current is decoupled into *d* and *q* axis, and thus they can be controlled independently.

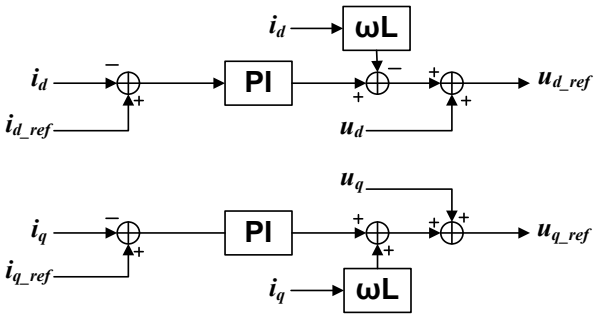

Fig. 6. PI Controller with feed forward compensation.

Fig. 6 demonstrates the PI controller with feed forward compensation. Voltage and frequency droop control method can be defined as (Guerrero et al., 2011):

$$\begin{aligned} \omega &= \omega^* - m\left(P - P^*\right) \\ V &= V^* - n\left(Q - Q^*\right) \end{aligned} \tag{9}$$

where P^* and Q^* are the reference real and reactive power, ω^* and V^* are the grid rated angular frequency and voltage amplitude, ω and *V* are the references, and *m* and *n* are the slopes of the droop characteristics. The strategy of droop control is that each DG shares the power demand according to its own droop characteristic functions. The droop characteristic is shown in Fig. 7.

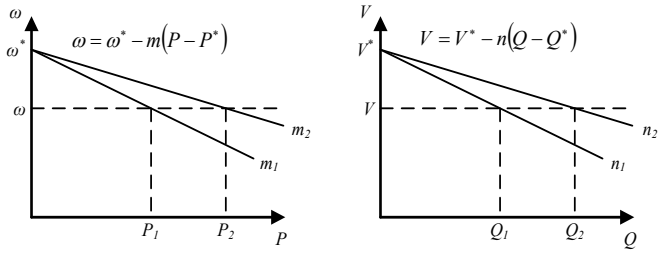

Fig. 7 Droop characteristics.

Fig. 7 shows that DGs allocate power according to the new stable working point at ω and *V* and the DG with steeper slope will share less power. Figs. 8 and 9 represent the schematic of droop control and details of 'Voltage Formation' block. The flow of real power is linearly dependent on the phase angle difference, and the reactive power flow is linearly dependent on the voltage magnitude difference (Katiraei and Iravani, 2006; Guerrero et al., 2006).

As shown in Fig. 8, the measured P and Q, reference P^* and Q^*, nominal f^* and V^* are considered as the input to calculate the reference $f_{\_ref}$ and $V_{\_ref}$ in 'droop control' block. u_{d_ref} and u_{q_ref} are reference voltage at d and q axis respectively after 'voltage formation' block.

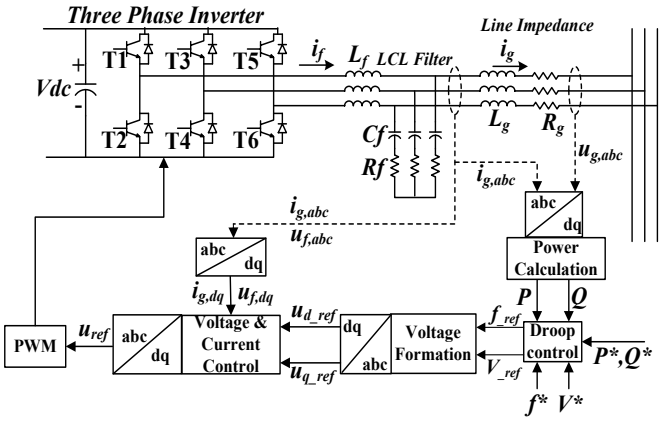

Fig. 8. Schematic of the droop control.

In Fig.9, f^* and V^* are grid rated frequency and voltage magnitude, respectively. f_{ref}, and V_{ref} are reference frequency and voltage magnitude, and they are obtained by droop control characteristic. Three-phase u_{ref} is obtained by voltage formation device and then converted into u_{d_ref} and u_{q_ref} by Park's transformation.

4. CASE STUDY

Test of controllers are carried out on Matlab/Simulink. Different scenarios have been studied in order to test the effectiveness of the proposed control strategies.

4.1 Simulation Parameters

As shown in Fig. 1, under grid connection mode PV and DG were operated by PQ control, meaning that they were told to generate exact real and reactive power according to their respective references. Under island mode, PV and DG were operated by droop control, meaning that when load changes, both DGs will automatically allocate power according to predefined droop characteristics. Parameters such as line impedance, rated power, voltage level, transformer setting, load, and control parameters are listed in Table 1.

Table 1. Simulation Parameters

Load1	P = 40kw, Q = 10kvar
Load2	P = 40kw, Q = 5kvar
Load3	P = 20kw, Q = 5kvar
DG	P_{rated} = 60kw, V_{dc} = 800V
PV	P_{rated} = 80kw, V_m = 680V, I_m = 280A
LC filter(PV)	R_f = 0.01 Ω, L_f = 0.6mH, C_f = 1500μF
LC filter(DG)	R_f = 0.5 Ω, L_f = 0.6mH, C_f = 2000μF
Line Z	R_L = 0.35 (Ω/km), X_L = 0.23(Ω/km)
Transformer	Y-Y: 208:13.8×10^3 V, R = 1%, X=4%
Droop control	1/m$_1$ = 10^{-5}, 1/n$_1$ = 10^{-5}, 1/m$_2$ = 0.3×10^{-5}, 1/n$_2$ = 0.3×10^{-5}

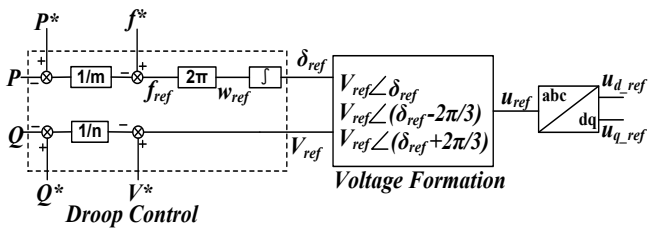

Fig. 9. Details of droop control and voltage formation.

4.2 Simulation Results

To verify the effectiveness of the PQ and droop control, grid-connected and island mode were simulated for controller testing. In grid-connected mode, microgrid was operating with the PQ control. The P, Q reference for PV was 70kw and 30 kvar, respectively, and P, Q reference for DG was 40kw and 10 kvar. Fig. 10 demonstrates the control results.

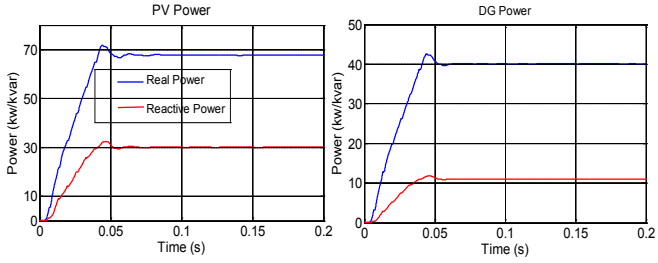

Fig. 10. PQ control under grid-connected mode.

As shown in Fig. 10, both controllers for PV and DG have quick responses and track the references effectively. Note that real and reactive power can be controlled independently because of the decoupling of the reference current (8). Fig. 11 illustrates the case that microgrid was operating by droop control under grid-connected mode in the beginning but disconnected from the grid at 4 second, and reconnected to the grid at 7 second. Fig. 12 illustrates the case that microgrid was operating at island mode by droop control in the beginning and load 3 disconnected at 4 second, and yet reconnected to the grid at 7 second.

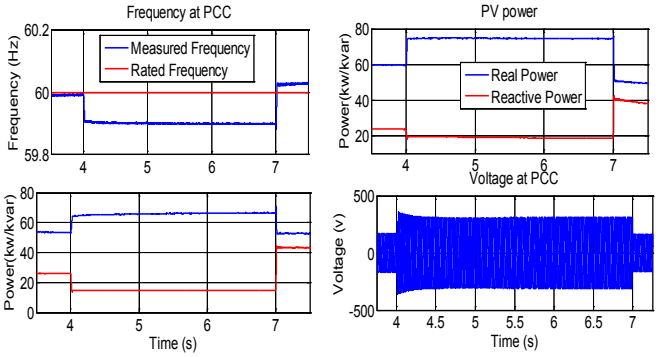

Fig. 11. Droop control for switching modes.

From Fig. 11, frequency at PCC decreases as microgrid disconnected from the grid at 4 second because the real power generation of PV and DG increase in order to match load demand and as the droop characteristics defined in Fig.

7, frequency will decrease. The voltage at PCC increases as microgrid disconnected from grid, because the reactive power of both DGs (Fig. 7) decrease, meaning that the grid was absorbing reactive power from micrigrid while connected. At 7 second when microgrid is reconnected to the grid, frequency increases as real power decreases and voltage decreases as reactive power increases.

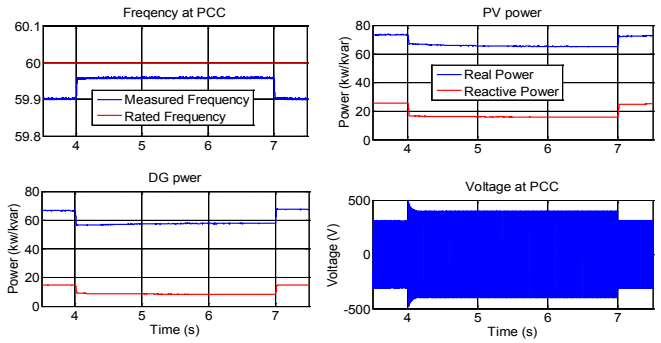

Fig. 12. Droop control for varying load.

From Fig. 12, frequency at PCC is not at rated value when microgrid is operating in island mode. At 4 second load 3 is disconnected from microgrid, and the frequency increases because the total power generation decreases to match the load demand. The voltage at PCC increases because the reactive power decreases as well. At 7 second, when load 3 is reconnected to the microgrid, the real and reactive power generation of both DGs increase in order to meet the load demand, therefore the frequency and voltage decrease. Both cases have shown that the droop controller works effectively in terms of reallocating power sharing between two DGs and fast responding to load changes while maintaining the frequency and voltage at acceptable level.

5. CONCLUSIONS AND FUTURE WORK

In this paper a detailed PV model with MPPT, and PQ and droop controllers is developed for inverter interfaced DGs. The use of PQ control ensures that DGs can generate certain power in accordance with real and reactive power references. Droop controller is developed to ensure the quick dynamic frequency response and proper power sharing between DGs when a forced isolation occurs or load changes. Compared to pure V/f control and master-slave control, the proposed control strategies which have the ability to operate without any online signal communication between DGs make the system operation cost-effective and fast respond to load changes. The simulation results obtained shows that the proposed controller is effective in performing real and reactive power tracking, voltage control and power sharing during both grid-connected mode and islanded mode.

To fully represent the complexity of the microgrid, future work will include the development of hierarchical controllers for a microgrid consisting of several DGs and energy storage system. The function of primary controller is to assign optimal power reference to each DG to match load balances and the secondary controllers are designed to control local voltage and frequency.

REFERENCES

Barsali, S., Ceraolo M., Pelacchi, P., and Poli, D. (2002). Control techniques of dispersed generators to improve the continuity of electricity supply. *IEEE Conf., Power Engineering Society,* vol.2, pp.789-794.

Cai, N., and Mitra J. (2010). A decentralized control architecture for a microgrid with power electronic interfaces. *IEEE conf., North American Power Symposium,* pp. 1-8.

Chen, X., Wang, Y.H., and Wang, Y.C. (2013). A novel seamless transferring control method for microgrid based on master-slave configuration. *IEEE Conf., ECCE Asia*, pp. 351-357.

Cho, C. H., Jeon, J.H., Kim, J.Y., Kwon, S., Park, K., and Kim, S. (2011). Active synchronizing control a microgrid. *IEEE Trans., Power Electron.*, vol. 26, no. 12, pp. 3707-3719.

Choi, J.W. and Sul, S.K. (1998). Fast current controller in three-phase AC/DC boost converter using d-q axis cross-coupling. *IEEE Trans., Power Electron.,* vol.13, no.1, pp. 179-185.

Guerrero, J.M., Vasquez, J.C., Matas, J., Vicuna L.G., and Castilla, M. (2011) Hierachical Control of Droop-Controlled AC and DC microgrid-A general approach toward standardization. *IEEE Trans., Industrial Electron.,* vol. 58, no.1, pp. 158-172.

Hatziargyriou, N., Asano, H., Iravani, R., and Marnay, C. (2007). Microgrids. *IEEE Power&Energy Magiazine,* July-Aug. 2007 vol.5, no.4, pp. 78-94.

Kundur, P. (1993). Power system stability and control. McGraw-Hill, New York.

Peng, S.J., Luo, A., Lv Z.P., Wu, J.B., and Yu, L. (2011) Power control for single-phase microgrid based on the PQ theory. *IEEE conf. Indust., Electron., and Applications,* pp. 1274-1277.

Puttgen, H.B., MacGregor, P.R., and Lambert, F.C. (2003). Distributed generation: semantic hype or the dawn of a new era? *IEEE Power&Energy Magiazine,* Jan-Feb 2003, vol.1, no.1, pp. 22-29.

Ropp, M. E., and Gonzalez, S. (2009) Development of a Matlab/Simulink Model of a single-phase grid-connected photovoltaic system. *IEEE Trans., Energy Conversion*, vol. 24 no.1, pp.195-202.

Saurav S. (2012) *Photovoltaic power control using MPPT and boost converter.* Bachelor Thesis, National Institute of Technology, Rourkela

Tan, K.T., So, P.L., and Chu, Y.C. (2010). Control of parallel inverter – interfaced distributed generation systems in microgrid for islanded operation. *IEEE Conf., Probabilistic Methods Applied to Power Systems*, pp.1-5

Villalva, M. G., Gazoli, J. R., and Ruppert, F. (2009). Comprehensive approach to modelling and simulation of photovoltaic arrays. *IEEE Trans., Power Electron.,* vol.25 no. 5, pp. 1198-1208.

Wu, B., Liang Y.Q., Zargari, N., and Kouro, S. (2011). Power conversion and control of wind energy systems. Wiley, New Jersey.